Grant agreement no. 243964

QWeCI

Quantifying Weather and Climate Impacts on Health in Developing Countries

D3.1d – Regional seasonal predictions, with uncertainty estimations, in the target regions, and inclusion in the QWeCI Statistical Downscaling Portal, accessible to partners in user–friendly formats

Start date of project: 1ˢᵗ February 2010

Duration: 42 months

Lead contractor: CSIC
Coordinator of deliverable: CSIC
Evolution of deliverable

Due date :   M24
Date of first draft :   15 July 2012
Start of review :   17 September 2012
Deliverable accepted :   19 September 2012

Project co-funded by the European Commission within the Seventh Framework Programme (2007-2013)		
Dissemination Level		
PU	Public	
PP	Restricted to other programme participants (including the Commission Services)	PP
RE	Restricted to a group specified by the consortium (including the Commission Services)	
CO	Confidential, only for members of the consortium (including the Commission Services)	
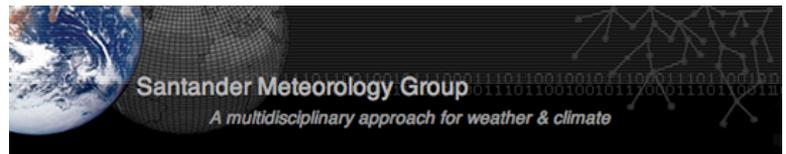
D3.1.d: Regional seasonal predictions, with uncertainty estimations, in the target regions, and inclusion in the QWeCI Statistical Downscaling Portal, accessible to partners in user-friendly formats

R.Manzanas[1], J.M.Gutiérrez[1], A.S.Cofiño[2], D.San-Martín[3], M.Tuni[3], S.Herrera[3]

[1] *Instituto de Física de Cantabria, CSIC-Universidad de Cantabria, Spain*
[2] *Universidad de Cantabria, Spain*
[3] *Predictia Intelligent Data Solutions, Spain*
correspondence: rmanzanas@ifca.unican.es; gutierjm@unican.es

version:1. *July 2012*

Abstract

Regionalized seasonal predictions of maximum temperature and precipitation for a set of selected stations within the QWeCI countries were obtained using state-of-the art statistical downscaling methods (analogs, regression, and GLMs). First, the downscaling methods were calibrated under the Perfect Prognosis approach, that is, ERA-Interim reanalysis was used as predictor data, identifying the optimum predictors for each variable in each region. Then, the resulting statistical methods were applied to the outputs of the ENSEMBLES Stream 2 multi-model experiment. The skill of the Stream 2 raw and downscaled predictions was evaluated and compared against the Perfect Prog. results, considered as the limit of attainable skill. Uncertainties associated with the different models, downscaling methods and predictor datasets were also assessed. Finally, the experiments here presented are available through the QWeCI downscaling portal, where users can downscale the regional projections or even try alternative downscaling experiments in an interactive way.

1 Introduction

Global Forecast Systems (GFSs) are unable to provide information at the spatial scale required by many stakeholders. Hence, regionalisation/downscaling methods are necessary for transferring the global predictions to smaller (regional or local) spatial scales, providing predictions calibrated and adapted to the required scale. Statistical Downscaling (SD) is the most popular approach in seasonal forecasting, due to the enormous amount of hindcasts to be downscaled for model calibration. In the perfect prognosis approach, statistical downscaling is based on empirical relationships derived between a set of predictands (observations of the target variable, such as precipitation), and a set of suitable large-scale predictors from a reanalysis dataset (such as sea level pressure). The resulting methods are latter applied to global seasonal predictions obtaining adapted local forecasts.

The present deliverable is a follow on of D3.1.b (QWeCI Statistical Downscaling Portal established and open to partners with an initial set of statistical-based seasonal predictions for the target regions, with documentation and support on good practices of use). Optimum predictors and downscaling methods are obtained for each of the QWeCI countries, and regional seasonal predictions using the resulting methods are provided for QWeCI partners through the QWeCI statistical downscaling portal[1], described in D3.1.b.

---

[1]https://www.meteo.unican.es/downscaling/qweci

2 Data

This deliverable focus on the performance of different SD methods to downscale temperature and precipitation in the QWeCI counties. In this section we describe the data used in this work.

2.1 Predictands (observations)

The QWeCI downscaling portal includes the whole MIDAS_QWeCI, GSOD_QWeCI, SenegalMet and GMet observational datasets described in D3.1.b to perform downscaling experiments in the QWeCI countries: Senegal, Ghana and Malawi. In order to illustrate the downscaling results in the present deliverable we follow the indications of deliverable D3.1.b and consider only some stations with best quality and longest records from the three latter datasets (the selected stations are shown in Fig. 1 and Table 1). Note, however, that the downscaling portal allows applying the resulting methods to any available dataset.

The seasons considered in the study are JFM, AMJ, JAS and OND. However, for the sake of brevity, and taking into account the strong climate seasonality in the pilot countries, only some key seasons have been analyzed in detail, although the results are available in the portal for all the seasons. Since
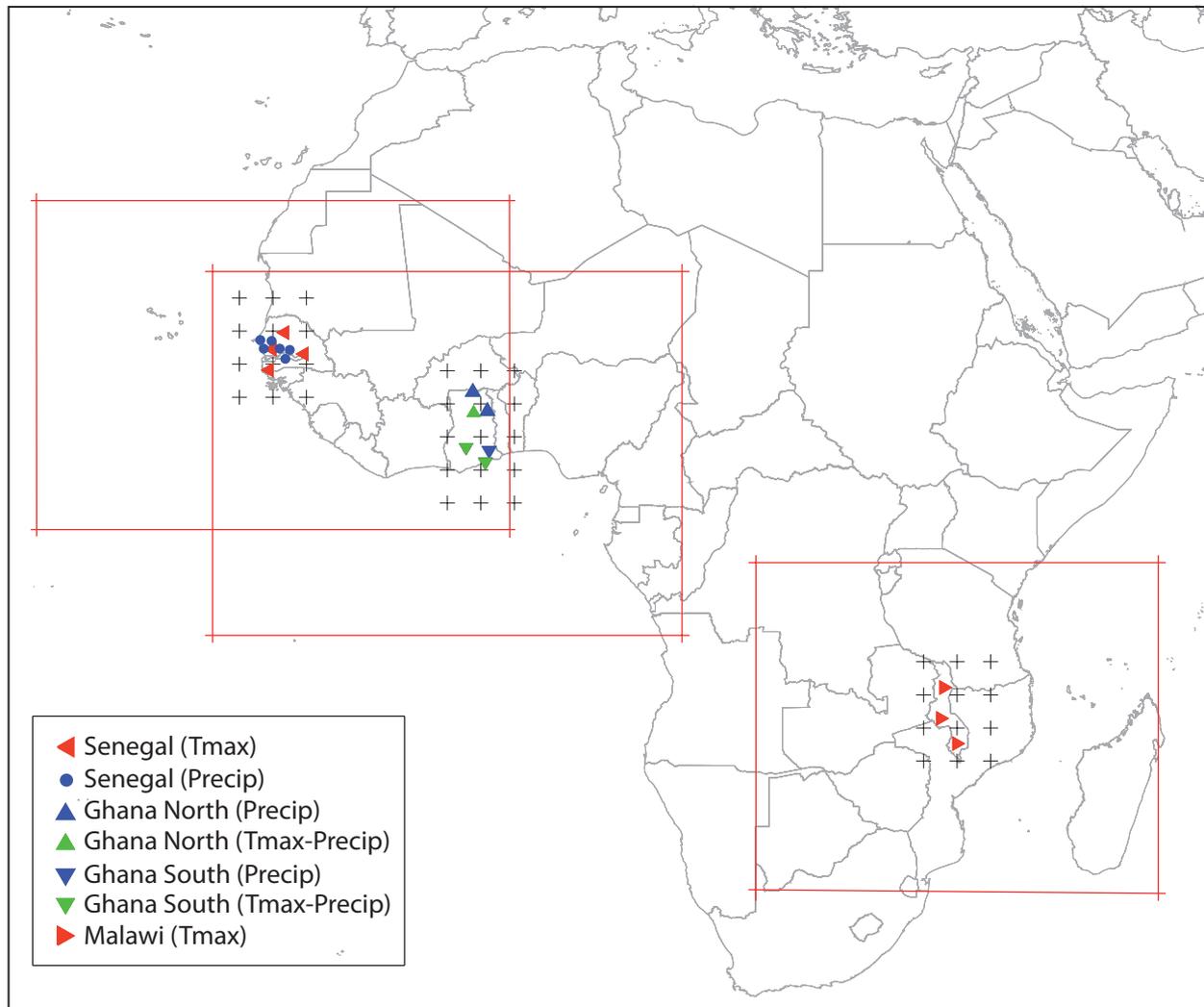
Figure 1: Stations considered for downscaling. Red/blue/green triangles represent stations where observed maximum temperature/precipitation/both maximum temperature and precipitation are available. Note that Ghana stations have been divided into two homogeneous (in terms of seasonal cycles) subgroups (North and South). Black crosses represent the initial grids considered in the downscaling process, whereas red squares represent the largest allowed domain of the optimization process in each are (later explained trough the text).

precipitation is more complex and difficult to predict than temperature, the seasons of study were selected based on precipitation regimes rather than on temperature ones. Figure 2 shows the climograms for the stations and seasons considered in each country. Note that for Ghana two different regions were defined (North and South), in order to gain homogeneity due to the different precipitation regimes.

In Senegal, climate is conditioned by its tropical latitude and the seasonal migration of the Inter Tropical Convergence Zone (ITCZ), as well as by other phenomena as the African Easterly Jet (AEJ) or the African Easterly Waves (AEWs). From January to March ITCZ is located south of Senegal, moving northward from April and covering all the country around July-August. The position of the ITCZ determines the prevailing winds. On the one hand, the trade winds are dry winds that originate in the continental interior and blow northeast. In winter and spring, when they are strongest, they are known as the harmattan (or dry monsoon). They bring no

precipitation apart from a very light rain, the heug. On the other hand, the moist maritime winds blow primarily from the west and northwest, bringing rains from June to September. Therefore, the country presents a marked dry-wet annual regime as shown in the climograms in Fig. 2. The length of the rainy season varies from five and a half months in the south to two and a half months in the north.

Note that the six stations considered for precipitation are located in nearby latitudes (see figure 1) and thus all of them present similar seasonal cycles (see figure 2), with a clear unique monsoon peak in JAS. Therefore, JAS was the only season considered for downscaling in Senegal (see table 1). The four stations considered for maximum temperatures also present similar seasonal cycles, with highest temperatures occurring in two seasons, AMJ and OND, and lowest in JAS. The average temperature in Senegal increases from the coast to the interior. On average, values are between 24 and 29 °C.

Senegal

Tmax	*Dataset (Stations)*	GSOD_QWeCI (Kaolack, Linguere, Tambacounda, Ziguinchor)
Precipitation	*Dataset (Stations)*	Senegal (Fatick, Gossas, Kaffrine, Koungheul, Nioro, Thies)
	Season (Period)	JAS (1979-2000)

Ghana North

Tmax	*Dataset (Stations)*	GMet (Tamale)
Precipitation	*Dataset (Stations)*	GMet (Navrongo, Tamale, Yendi)
	Season (Period)	JAS (1979-2000)

Ghana South

Tmax	*Dataset (Stations)*	GMet (Accra, Kumasi)
Precipitation	*Dataset (Stations)*	GMet (Accra, Akuse, Kumasi)
	Season (Period)	AMJ (1979-2000)

Malawi

Tmax	*Dataset (Stations)*	GSOD_QWeCI (Chileka, Lilongwe Int L'Airport, Mzuzu)
Precipitation	*Dataset (Stations)*	—
	Season (Period)	JFM (1983-1994)

Table 1: Stations, seasons and period of study considered for each zone and predictand in this study.
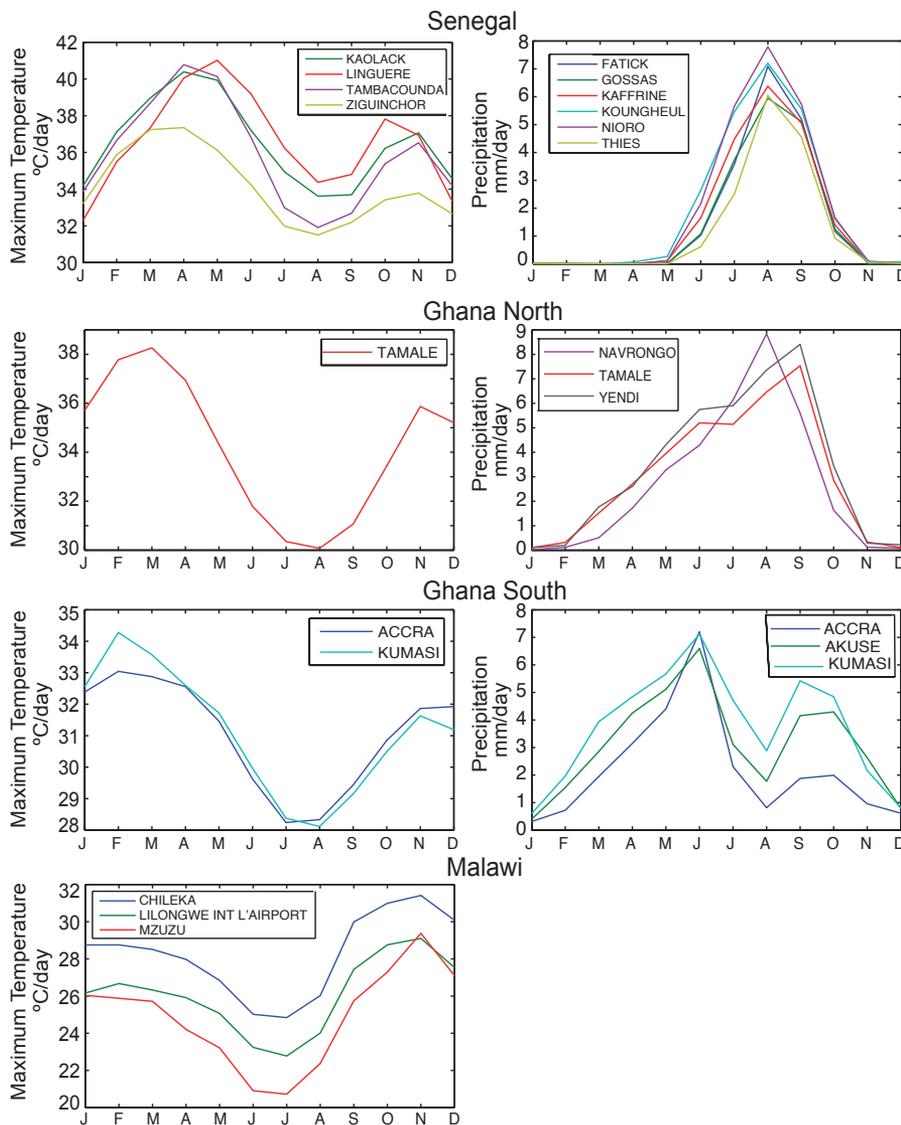
Figure 2: Maximum temperature/precipitation monthly climograms (upper/bottom row) for the stations considered in each zone (columns), in units/day.

Ghana presents a tropical climate marked by warm to hot temperatures throughout the year and abundant seasonal rainfalls. On the one hand, temperatures are hotter in the north than in the south, due to its longer distance from the modulating action of the ocean. The warm season occurs in JAS, whilst maximum temperatures are recorded in the start and the end of the year. On the other hand, rain in the northern part of the country is closely linked to the West African monsoon (thus to the position of the ITCZ, the AEJ and the AEWs, as occurs in Senegal), taking place around JAS. However, in the south, rainfall is more related to the sea surface temperatures (SSTs) in the Gulf of Guinea and it is more distributed throughout the year, falling mainly in two seasons: May-June and around October. Due to this marked difference between the north and the south climates, both for temperature and precipitation, we split the GMet stations into two homogeneous subgroups, called Ghana North and Ghana South (see figure 2). According to the main precipitation peak, JAS (AMJ) was the season considered for downscaling in Ghana North (Ghana South).

Malawi has a sub-tropical climate, relatively dry and strongly seasonal. There is a cool and dry season from May to October with mean temperatures varying between 17 and 27 °C and a warm and wet season stretching from November to April, during which 95% of the annual precipitation takes place. Although the range of observed temperatures is spread for the three stations considered, all of them present similar seasonal cycles (see figure 2). Since January to March are the most rainy months in Malawi, JFM was the season considered for downscaling. Due to the lack of observational records for precipitation, maximum temperature was the only variable treated in this country.

2.2 Potential Predictors

A list of potential predictors for the QWeCI regions was initially determined from the literature appeared in the last two decades. Most of them were focused on West African monsoon, the most interesting phenomena due to its large impact on human sectors. In the following, we present a brief summary of some of the most relevant published works, chronologically ordered, indicating the most important relationships found between large scale predictors and West African monsoon precipitation:

- Fontaine (1995) found that U and V at 200 and 850 hPa were the best predictors for August rainfall in the Sahelian and Guinean regions.
- Eltahir (1996) highlighted the importance of boundary-layer entropy at 1000 and 950 hPa, vorticity at 200 hPa and SST in the South Eastern Tropical Atlantic (SETA) region to predict monthly rainfall in West Africa.
- Zheng (1999) stated a teleconnection (well-known today) between Tropical Atlantic SSTs and the dynamics of the West African monsoon.
- Deme (2002) found that thermodynamical indices such as the lifting condensation level at 1000 hPa, U at 850 hPa, vorticity at 700 hPa and mixed indices such as

water vapor fluxes were the best predictors for August daily rainfall at Dakar.
- Rotstayn (2002) identified U at 900 hPa as the best predictor for July-August daily rainfall in the Sahel region.
- Mo (2002) used global SSTs and 200 hPa streamfunction with zonal means removed (PSI) to predict summer rainfall over the Sahel.
- Rowell (2003) indicated that averaged SSTs in the Mediterranean, the moisture flux, Q, U and V at 700 and 850 hPa affected JAS rainfall in the Sahel.
- Penlap (2004) found that relative humidity and U at 850 hPa (Q at 500 hPa and divergence at 700 hPa) provided the best link to the variability of local precipitation in northern (southern) Cameroon for March-June.
- Paeth (2005) analyzed how Tropical Atlantic SSTs, the AEJ, the AEWs, the Tropical Easterly Jet (TEJ), the Subtropical Jet (STJ) and the position of the ITCZ governed daily rainfall variability in West Africa.
- Moron (2008) suggested that predictors for JAS daily rainfall over Senegal must be selected to represent the three distinct vertical levels of the monsoon circulation, that is, the low-level monsoon flow (U and V at 925 hPa), the AEJ (U and V at 700 hPa) and the TEJ (U and V at 200 hPa).

Apart from the aforementioned studies, colleagues from UCAD (Senegal) and KNUST (Ghana) gave us some recommendations on the large scale variables dominating climate variability over West Africa. In summary, they recommended us to look at the following predictors:

- U, V and T at 600-700-850 hPa. Wind vorticity and temperature at these levels determines the AEJ activity. Within the jet, maximum wind speeds are located at around 600 hPa. The AEJ is considered to play a crucial role in the West Africa monsoon and helps to form the AEWs. Convective cells associated with these waves can form tropical cyclones and squall lines (lines of severe thunderstorms that can form along or ahead of a cold front) after they move from West Africa into the tropical Atlantic, mainly during August and September.
- U, V and Q at 850-925 hPa. Winds and humidity at these levels characterize the type of prevailing winds in the low troposphere; the trade winds that suppresses the monsoon or the moist maritime winds blowing bringing monsoon precipitation.

The variables resulting from this study form the list of potential predictors to be used in the project.

2.3 Model Data (Reanalysis and GFSs)

On the one hand, we used ERA-INTERIM[2] (Dee, 2011), the latest atmospheric reanalysis produced by the European Centre for Medium-Range Weather Forecasts (ECMWF), to obtain the predictors in the Perfect Prognosis (PP) case. ERA-INTERIM covers the period 1979 to date and it is expected

---

[2]http://www.ecmwf.int/research/era/do/get/era-interim

Centre	Atmospheric model and resolution	Ocean model and resolution
ECMWF	IFS CY31R1 (T159/L62)	HOPE ($0.3°-1.4°$/L29)
IFM-GEOMAR	ECHAM5 (T63/L31)	MPI-OM1 ($1.5°$/L40)
CMCC-INGV	ECHAM5 (T63/L19)	OPA8.2 ($2°$/L31)
MF	ARPEGE4.6 (T63)	OPA8.2 ($2°$/L31)
UKMO	HadGEM2-A (N96/L38)	HadGEM2-O ($0.33°-1°$/L20)

Table 2: Overview of the five seasonal models conforming to the Stream2 multi-model experiment of the EU project EMSEMBLES: The UK Met Office (UKMO), Meteo France (MF), the European Centre for Medium-Range Weather Forecasts (ECMWF), the Leibniz Institute of Marine Sciences (IFM-GEOMAR) and the Euro-Mediterranean Centre for Climate Change (CMCC-INGV).

to perform better than the preceding ERA40 over the countries of study, due, among others, to its enhancements in data assimilation and use of observations.

On the other hand, we considered the state-or-the-art seasonal hindcast provided by the Stream2 multi-model experiment of the EU-funded ENSEMBLES project[3], including the global atmosphere-ocean coupled models shown in Table 2. The atmosphere and the ocean were initialized four times a year within the period 1960-2005 (starting the first of February, May, August and November) producing seven month-long hindcasts (see Weisheimer, 2009, for more details about the experiment). Each model ran an ensemble of nine initial conditions (nine members) produced perturbing the realistic estimate of the observed initial state (the analysis). Since the seasons of study considered in this deliverable were JFM, AMJ and JAS, only two months lead-time predictions were analyzed, that is, initializations of November/February/May were used to downscale seasons JFM/AMJ/JAS, respectively. Note, however, that the whole set of hindcasts is available through the QWeCI downscaling portal for further analysis.

Since ERA-Interim and the five ENSEMBLES Stream2 models (see Table 2) have different resolutions, all datasets were regridded to the same $2.5°$ regular grid using bilinear interpolation. Thus, the finer resolution of ERA-Interim is not fully exploited in this work, since the resulting statistical downscaling methods would not be applicable to the seasonal forecasting outputs.

Unfortunately, not all the variables corresponding to the potential predictors identified in Sec. 2.2 are available for the ENSEMBLES Stream2 seasonal models used in this work[4]. Therefore, we only considered those variables/levels available for both ERA-Interim and ENSEMBLES Stream2 datasets. The resulting list of variables is shown in Table 3. Note that this lack of data could imply a foreseeable loss of skill since, for instance, the 600-700 hPa levels available in ERA-Interim, which are closely related to West African precipitation, are not available in ENSEMBLES Stream2 — although they are in ERA-Interim— and, thus, are discarded in this study.

---

[3]http://www.ecmwf.int/research/EU_projects/ENSEMBLES

[4]Note that storing all the variables available for ERA-Interim is virtually impossible for a multi-model seasonal hindcast experiment since the volume of data increases two orders of magnitude: 5 models, 9 members, four initializations.

3 Downscaling Methods

Different statistical methods have been proposed in the literature to adapt the coarse predictions provided by global forecast systems to the finer scales required by impact studies. The different statistical downscaling techniques are broadly categorized into two classes:

- *Weather typing (analogs)*, based on nearest neighbors or in a pre-classification of the reanalysis into a finite number of weather types obtained according to their synoptic similarity; these methods are usually non-generative, since they consist of an algorithmic procedure to obtain the prediction, such as the method of analogs.
- *Transfer functions (regression)*, based on linear or nonlinear regression models to infer the relationships between predictands and the large-scale predictors; these methods are "generative" in the sense that the projections are derived from a model obtained from data. These techniques include linear regression (typically used for temperature), Generalized Linear Models (GLMs, typically used for precipitation) and more flexible —but computationally expensive— neural networks.

In the present study we have tested two representative statistical downscaling techniques for maximum temperature and precipitation. On the one hand, an analog downscaling technique (based on the closest analog, using the Euclidean distance) was considered for both variables. On the other hand, a multiple linear regression was considered for temperature whereas a GLM was used for precipitation; in both cases, in order to reduce the dimensionality of the predictors, the n PCs explaining the 95% of the variance were considered as input for the regression models (note that n is different for each predictor dataset and domain combination, but a maximum of 30 PCs was obtained in the most complex configurations). In all cases, the predictor datasets were firstly standardized, gridbox by gridbox. Note that, besides allowing for a better combination of different predictors for the downscaling process, the standardization process removes the effect of the systematic biases of the seasonal models.

In order to obtain the optimum configuration of predictors and geographical domains for each of the above downscaling techniques in each of the regions, we implemented an automatic stepwise-like greedy procedure (hereafter referred to as OPTimizer Algorithm, OPTA) which iteratively test new predictors (from the list of predictors shown in Ta-

Code	Name	Level (hPa)	Time	Units
Z	Geopotential	850,500,200,50	00 UTC	m^2s^{-2}
T	Temperature	850,500,200,50	00 UTC	K
U	Zonal wind	850,500,200,50	00 UTC	ms^{-1}
V	Meridional wind	850,500,200,50	00 UTC	ms^{-1}
Q	Specific humidity	850,500,200,50	00 UTC	$kgkg^{-1}$
2T	2-meters temperature	0 (2 meters)	00 UTC	K
MSL	Mean sea level pressure	0 (mean sea level)	computed from 6,12,18,24 UTC	Pa
10U	Zonal comp. of 10m wind	0 (10 meters)	00 UTC	ms^{-1}
10V	Meridional comp. of 10m wind	0 (10 meters)	00 UTC	ms^{-1}
TP	Total precipitation	0 (surface)	daily accumulated from 00 UTC	*m of water*
MX2T	Maximum temperature	0 (2 meters)	computed from 6,12,18,24 UTC	K
MN2T	Minimum temperature	0 (2 meters)	computed from 6,12,18,24 UTC	K

Table 3: ERA-Interim and ENSEMBLES Stream2 variables available through the QWeCI portal.

ble 3) as well as new/modified geographical domains (starting with the domains marked with black crosses in Fig. 1, with largest allowed domains marked with the red squares), until an optimum configuration is obtained where no further improvement of the model performance is achieved. Different statistical scores were tested in order to measure model performance (bias, RMSE, MAE, correlation, and combinations of the above) obtaining similar results in all cases. Finally, we considered Pearson/Spearman correlation for temperature/precipitation, respectively[5]. In order to avoid model overfiting, for each zone the first 75% of the whole period of study was used for *training* and the last 25% for *test*. Seasons were treated separately, that is, only DJF data were used to calibrate methods which were later used to predict DJF.

As opposite to standard stepwise methods, OPTA performs two types of operations in the iterative search process: including predictors and extending the geographical domain. The type of the operation is chosen at random in each iteration and the algorithm proves all the possibilities. In the case of the predictors, the algorithm test all models resulting from the addition of an extra predictor; in the case of the geographical domains the algorithm test all possible domains resulting from increasing a 10% the size of the current domain in the north/south/east/west directions. Moreover, in order to discard unnecessary predictors, or allow domain reductions, the algorithm is implemented in a forward-backward form, and the inclusion/exclusion or extension/reduction character of the operation is also selected at random. In every single test within each iteration, the downscaling is done and results are validated against observations. The best configuration is retained for the next iteration in case that a performance improvement is obtained w.r.t. the value of the previous iteration (a 1% relative improvement is required). The algorithm stops when no improvement is obtained with any of the possible operations.

---

[5]Although the downscaling method works at a daily basis, the correlation was computed at a 10-day basis for precipitation, aggregating both observed and predicted data on 10-day blocks. This led to higher correlation values allowing to reduce the "noise" in the optimization process.

4 Results in Perfect Prog.

In this section we describe the results of the calibration of the statistical downscaling methods in PP conditions, i.e. using ERA-Int predictors. In this case, the period of study for the different zones is determined by the overlap between the reanalysis data and the observational records (see Table 1).

In order to obtain an initial estimation of the potential of the different predictors (shown in Table 3) for downscaling in perfect prognosis conditions, we computed the correlation of the available temperature and precipitation observations in each region and the different predictors from ERA-Interim (considering the neighboring gridbox for each station). The largest the correlation, the strongest the physical link is between the local predictands and the large-scale predictors, and thus the better the predictor is expected to be for downscaling. Figure 3 shows, the resulting correlations for each region (in rows) and variable (temperature on the left and precipitation on the right).

This figure show that marginal correlations between predictands and predictors are in general low, even between the observed variable and its corresponding reanalysis counterparts (TP, MX2T and MN2T, shown in the three first places of the graphs), with maximum values of 0.5-0.7 for temperature and 0.2-0.5 for precipitation, depending on the stations and regions. Surface temperatures are in general the most correlated with both observed maximum temperature and precipitation. T at 850 hPa is also quite correlated with maximum temperature in all zones. Q at 850 hPa, U at 850 hPa and V at 850 hPa and Q at 500 hPa are also significantly linked with this variable in Senegal, Ghana and Malawi, respectively. In addition, surface winds (U at 850 hPa) are related to precipitation in Senegal (Ghana South).

The above results show the low quality of the reanalysis over this region (note that in extra-tropical latitudes, as for instance occurs in Spain, ERA-INTERIM correlations are around 0.9 and 0.7 for temperature and precipitation, respectively). Therefore, the joint effect of different variables (co-factors) can be more relevant in this situation and, thus, finding the best combination of predictors and geographical
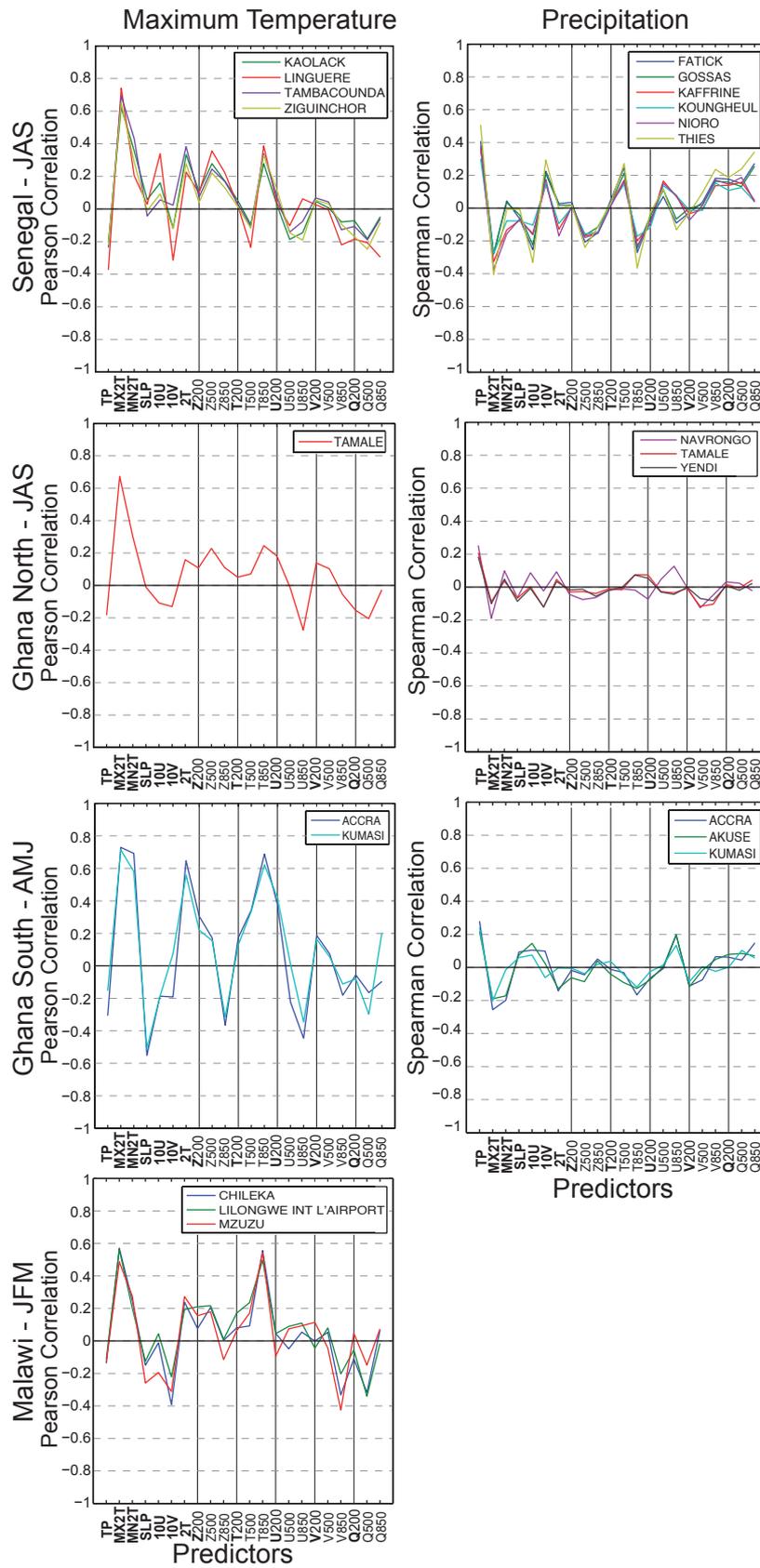
Figure 3: Pearson/Spearman correlation between observed maximum temperature/precipitation (in columns) and the ERA-INTERIM predictors considered at the nearest grid point. Different regions/seasons are represented in rows.

domain results in an exhaustive search of possible combinations. This was the reason that motivated the development of the OPTA algorithm, described in Sec. 3. A typical execution of this algorithm for an illustrative predictand (precipitation), region (Senegal) and season (JAS) is shown in Table 4; note that the optimum configuration is obtained in this case after four iterations (the last two iterations do not achieve any further improvement).

n	r	$Predictors$	PCs	X	S
0	-	-	-	-	-
1	0.248	U850	6	0:0	0:0
2	0.296	U850-Q850	13	0:0	0:0
3	0.347	U850-Q850	17	0:0	1:0
4	**0.376**	**U850-Q850-T500**	**23**	**0:0**	**1:0**
5	0.349	U850-Q850-T500	12	0:2	1:-2
6	0.361	U850-Q850-T500-U500	29	0:0	1:0

Table 4: Tracking of the optimization process for precipitation in Senegal in JAS, for the analog method. Each row corresponds to one iteration; columns (from left to right) indicate the iteration (n), correlation (r), predictor dataset, number of principal components explaining the 95% of variance, position of the left-bottom corner of the current domain with respect to the initial one (X, in gridboxes), and the increase (positive)/reduction (negative) of the current domain with respect to the initial one (S, in gridboxes).

The OPTA algorithm was applied to the different regions and seasons shown in Table 1. As in any iterative algorithm, the optimum reached might be a local one rather than the global one. To take this into account, the OPTA was run ten times for each experiment for a robust interpretation of the results and the best solution attained was selected in each case (it is worth noticing that the same, or similar, optimum predictors-domains were obtained in most of the instances). The resulting predictor datasets are shown in Table 5.

Senegal (JAS)

Tmax	an1	2T0-T850
	reg	2T0-T850-Q850-V500-Z850
Precipitation	an1	U850-Q850-T500
	glm	Q850-V850-Z850-T200

Ghana North (JAS)

Tmax	an1	V850-T850-Q200-U200
	reg	U850-2T0-V850-U500
Precipitation	an1	T850
	glm	U200-V850-Z200-U500

Ghana South (AMJ)

Tmax	an1	2T0-U850-Q850
	reg	2T0-SLP0
Precipitation	an1	2T0-T850
	glm	U850-U200-T850

Malawi (JFM)

Tmax	an1	T850-T500-V850-U850
	reg	T850-Q500-Z200
Precipitation	an1	
	glm	

Table 5: Final optimum predictor datasets considered for each zone/predictand/method. Analogs (an1), multiple regression (reg), and GLM (glm).

The first conclusion from the use of the OPTA was that the optimum domain/predictor dataset depended on the downscaling method considered. Despite this variability, is is important to notice the consistency between the predictor datasets found and the results reported in the literature, described in Sec. 2.2. For the case of precipitation, U at 200 and 850 hPa appeared among the most relevant predictors for Senegal and Ghana, which is in agreement with Fontaine (1995), Eltahir (1996), Mo (2002), Deme (2002), Rotstayn (2002), Rowell (2003) and Moron (2008). Q at 850 hPa also came up as an important predictor, as found in Rowell (2003) and pointed out by our QWeCI colleagues. The latter also suggested the importance of T at 850 hPa, which is systematically included in predictor datasets found for Ghana. Note also that, in relative agreement with the correlation analysis shown in Fig. 3, surface temperatures, which were shown to exhibit high correlations with precipitation in all zones, were among the predictors found for Ghana. In the same line of agreement, T at 850 hPa turned up as one of the most relevant predictors for maximum temperature in Senegal and Malawi. In addition, other ERA-Interim variables which were shown to be strongly correlated with maximum temperature appeared among the selected predictors: Q at 850 hPa in Senegal, U at 850 hPa in Ghana (both North and South), SLP in Ghana South and V at 850 hPa and Q at 500 hPa in Malawi. However, in contrast with the results of the correlation analysis, surface winds did not come up among the predictors found for Senegal, neither for maximum temperature nor for precipitation.

These results have been obtained considering only large-scale predictors, excluding surface variables poorly represented by the global models (or highly affected by model parameterization which might be different in the reanalysis and the different seasonal models). In particular we excluded TP, MX2T and MN2T as potential predictors, which are represented as a separate group in Table 3. Moreover, in order to test the performance of this type of predictors we also tested the so called MOS-like statistical downscaling configurations, including a single predictor (the model variable counterpart of the predictand, i.e. TP for precipitation and MX2T for maximum temperature) defined over the initial domains defined in Fig. 1. The results of the MOS-like configurations in the Perfect Prog. approach (using ERA-Interim outputs) will give a benchmark for the model performance. Moreover, the comparison of the results for the seasonal forecasts will allow us estimating the adequacy of this type of configuration for seasonal forecasting. These results are shown in the next section.

5   Results for Seasonal Forecats

The optimum configurations found in Sec. 4 (Table 5) were applied to the five seasonal forecast models shown in Table 2, considering the whole hindcast period 1960-2005. To this aim, the statistical downscaling methods were applied to the corresponding predictors for each of the model members, obtaining nine downscaled daily series for each model (one per member) for each of the stations. Afterwards the

nine members where averaged together at a seasonal level obtaining a single 45-years seasonal prediction for each of the models. These predictions where validated separately for each model considering also the multi-model mean, obtained by averaging the five model predictions. In this case, the validation was performed considering the observed and predicted yearly series for a period obtained as the intersection of the observational and hindcas years. Thus, we evaluate the skill of the models to capture the interannual variability of the corresponding season. In order to obtain a measure of the added value of the statistical downscaling technique we compute the performance of both the raw model outputs (maximum temperature, or precipitation) and the statistically downscaled values according to the different methods.

Figure 4 shows the results for the four regions defined for temperature (in columns). The first two rows show the Pearson correlation ρ for an illustrative model (the ECMWF model, first row) and for the multi-model (second row). The last row shows the Mean Absolute Error (MAE) for the multi-model prediction. For the raw model outputs, this score is highly influenced by the systematic model biases and, thus, allow us to evaluate the added value of the statistical downscaling techniques from this point of view. Each of the panels in the figure show the results for the different stations in the corresponding region. For instance, the panel in the upper left corner correspond to the correlation results for the ECMWF model for Senegal, containing four different stations. The results for each station are given by five colored bars corresponding to the raw model outputs (gray bar), ant to the analog and regression downscaled values considering the MOS-like and the optimum configuration (see the legend for details on colors). Therefore, the added value of the statistical downscaling methods can be evaluated by comparing the first bar with the remaining four ones (for different downscaling options); moreover, for each of the statistical downscaling methods (analogs and regression), the differences between the MOS-like configuration and the optimized one (containing only large-scale predictors) can be also established by comparing the results of the corresponding consecutive bars. Finally the bars show the results for the PP approach (considering the "perfect" predictors from ERA-Interim), whereas the corresponding results for the seasonal forecasting systems are indicated with a black square within each bar. Therefore, the color bars in the panels of the first two rows are exactly the same, since in both cases they are the results of considering ERA-Interim as predictor; note that this facilitates the comparison of the results for the illustrative model (ECMWF) and the multi-model.

In general, the results for the perfect model configuration (color bars) are quite homogeneous, attaining correlation between 0.6 and 0.8 in most cases, and for all downscaling methods and configurations. Thus, inter-annual variability is appropriately captured by the statistical downscaling methods. However, the results of the seasonal forecasting systems are much lower, particularly for Senegal and Ghana North. In those cases, the correlation of the direct model outputs (black square within gray bar) are much smaller than the corresponding to ERA-Interim (below 0.5 in all the stations, with the only exception of Kaolack), whereas it is comparable in Ghana South and, particularly in Malawi. The per-

formance of the seasonal models (as estimated by the direct model outputs) determine the posterior performance of the statistical downscaled values which yield similar correlations than the direct model outputs, with higher variability among downscaling methods and configurations for those cases with lower skill. However, the MAE results (the bias) are clearly better for the downscaled series than for the direct model outputs, influenced by the systematic model biases. Finally, an interesting result is that MOS-like configurations perform similarly to the optimized ones using only large-scale information in this case. The results from the multi-model predictions are, in general, better than the results of each individual model, in agreement with previous studies.

Figure 5 shows the results for precipitation. Note that in this case the scores are clearly poorer than for maximum temperature, with larger differences between the correlations for ERA-Interim and the seasonal forecast precipitation values (gray bars and black rectangle, respectively). The performance of the seasonal predictions is quite small, with correlations below 0.5 in almost all cases for both the direct model outputs and the downscaled values. Similarly to the previous case, in some cases the statistical downscaling methods allow reducing the bias (MAE) of the direct model outputs, thus adapting the predictions to the local scale, although they lack of skill to reproduce the annual variability. As opposite to the previous case, the MOS-like configurations are better in perfect prog. conditions (with ERA-Interim data), but the performance clearly degrades when using seasonal predictions from any of the global models. Therefore, MOS-like downscaling is not recommended for this variable.

Finally, in order to estimate the uncertainty of the results given by the different members (which were averaged in the previous results), Fig. 6 show two illustrative examples, for maximum temperature and precipitation, respectively. In this case, the raw ERA-Interim and model output are compared with the interval given by the nine ensemble members (45 for the multi-model), represented by a box-and-whiskers plot of the member values. It can be easily seen that the uncertainty is much larger for precipitation than for temperature. In the latter case, the inter-member variability is smaller than the inter annual signal, obtaining good correlations in all cases. However, in the former case the inter-member variability is larger than than the inter-annual one, shown the lack of a clear signal in this case. The figures over each of the panels show the correlation and MAE of the direct model output (first pair of values) and the for the downscaled results (using the mean of the ensemble, as given in the second pair of values).

6 The QWeCI downscaling portal

The resulting downscaled values for the different regions and variables have been included in the QWeCI downscaling portal (http://www.meteo.unican.es/downscaling/qweci) for the user/password qweci/qweci. For each region, both the analog and the regression methods are defined, using the optimum predictors found. Moreover, the user can define new config-
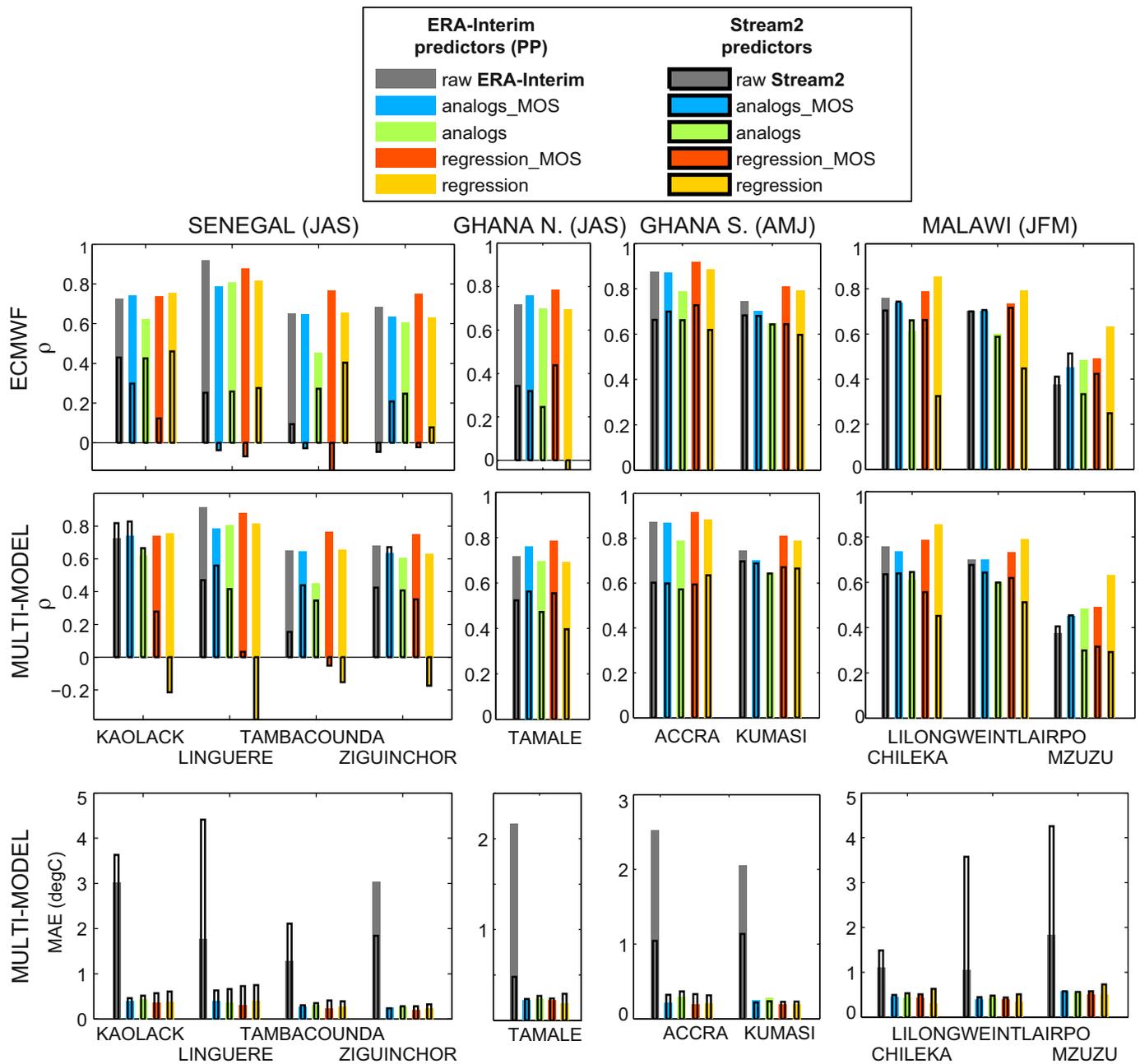
Figure 4: Results for the direct model outputs (gray bars) and the statistically downscaled results for four two different downscaling methods, each with two different configurations (color bars). The color bars show the perfect prognosis results, obtained using ERA-Interim as predictor; the corresponding black squares indicate the results for the seasonal forecasting systems, considering an illustrative model (the ECMWF model, first row), or the multi-model mean (second row). Mean Absolute errors are given in the third row. The results for the stations in different regions are given in different columns.
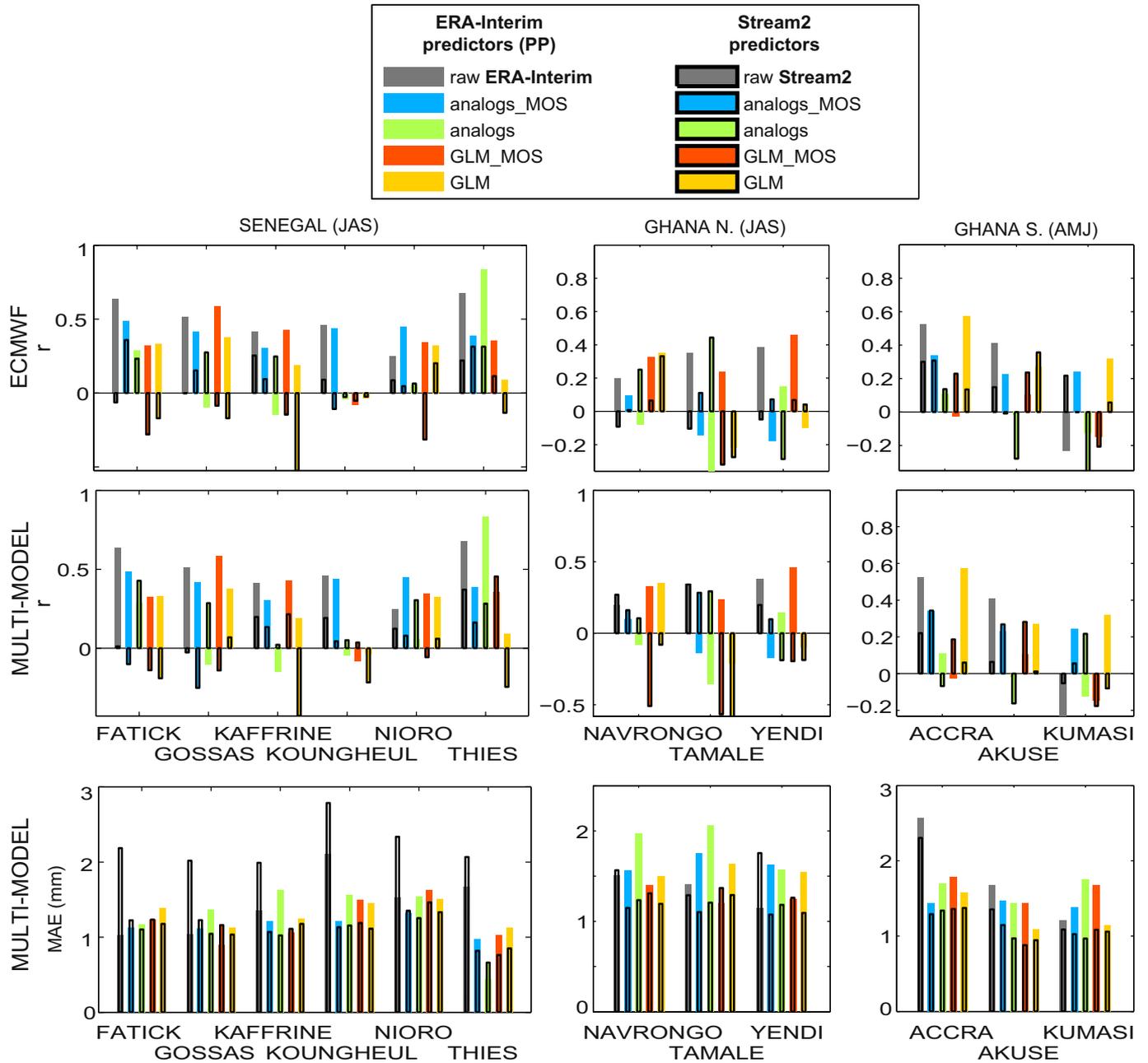
Figure 5: As figure 4, but for precipitation.
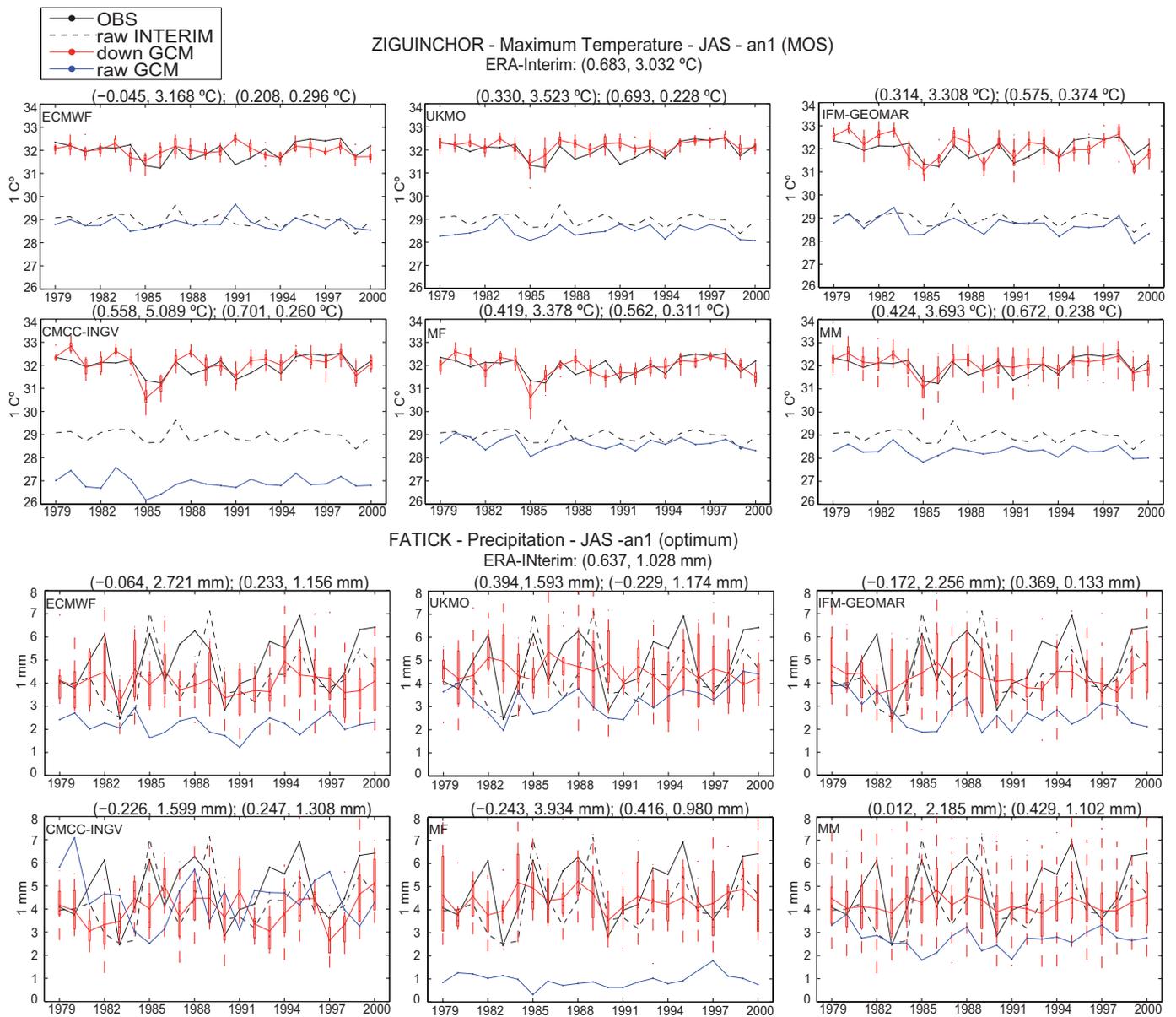
Figure 6: Illustrative example of the inter-member variability for two illustrative stations for maximum temperature (first two rows) and precipitation (last two rows). Each panel shows the results for a particular model, or for the multi-model.
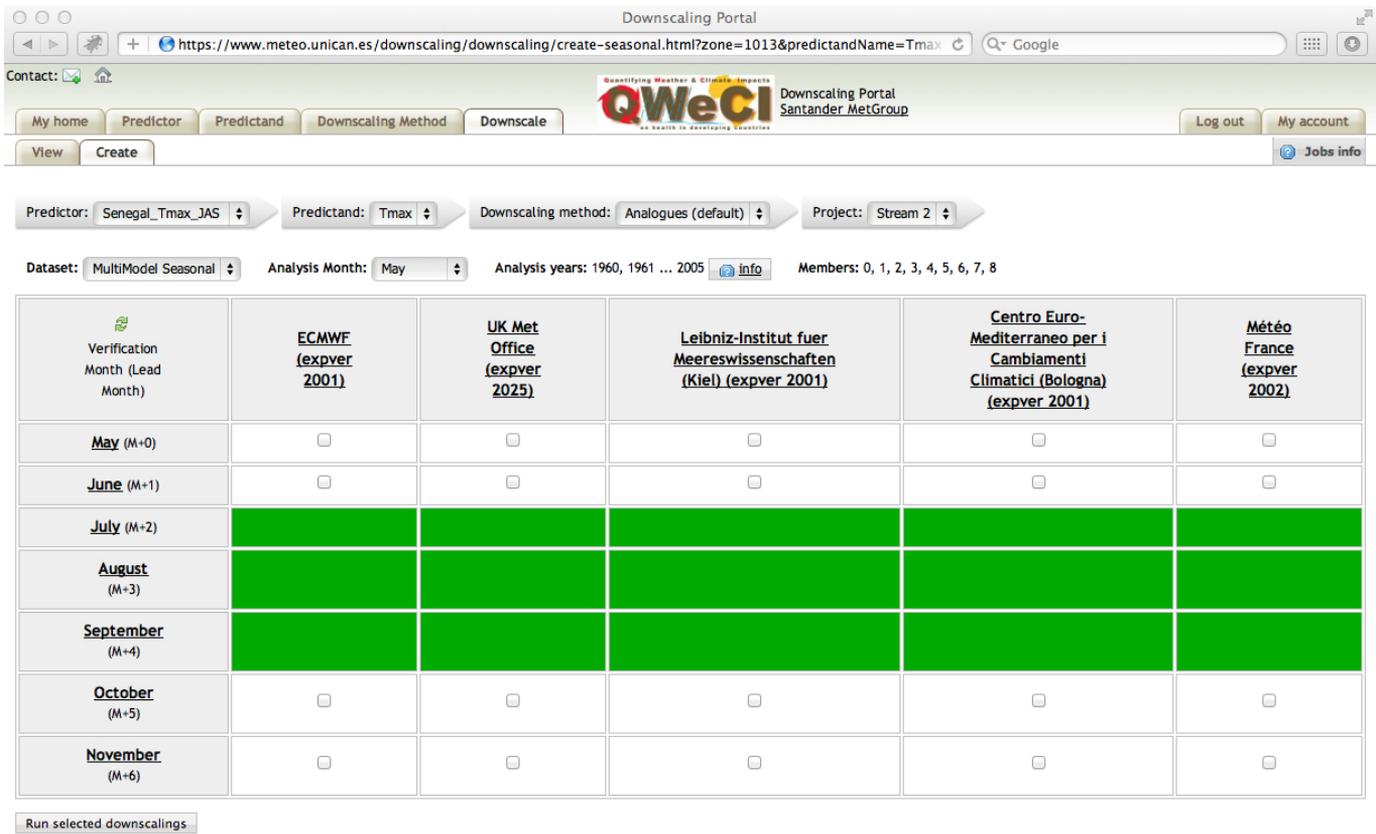
Figure 7: As illustrative example of the data produced and available in the QWeCI downscaling portal.

urations and methods, based on these results, using the portal facilities to to test and compare the performance of several approaches (note that the skill of statistical downscaling methods varies from variable to variable and from region to region). For a particular predictor and predictand, a particular downscaling method can be selected and configured from the "Downscaling Method" window, obtaining an automatic cross-validation[6]. This automatic validation feature is an important help for users for the iterative process of creating an appropriate predictor/domain configuration (variables, geographical domain, etc.).

For instance, Fig. 7 shows the available downscaled values for the Senegal_Tmax_JAS case, for the five available models with May initialization, including all members (9) and years (1960-2005). This information can be downloaded just by clicking on the corresponding checkboxes, marked as green in the figure.

7 Conclusions

Different downscaling methods have been tested for maximum temperature and precipitation in the QWeCI coun-

tries, considering different combinations of predictors and geographical domains. The downscaled values allow reducing the systematic biases present in the seasonal forecasting model outputs. However, the skill of the downscaled series for reproducing the inter-annual variability of the observed series rely on the skill of the forecasting system (characterized, e.g. by the skill of the direct model output). In general, good results are found for maximum temperature in some of the regions, whereas almost no skill is exhibited by both the direct model outputs and the downscaled series, in contrast with the results obtained in perfect model conditions using ERA-Interim.

The limited availability of data in the multi-model ENSEMBLES Stream2 dataset implies a foreseeable loss of skill since, for instance, the 600-700 hPa levels, which are closely related to West African precipitation, are not available in Stream2, although they are in ERA-Interim. Therefore, a potential gain of skill could be obtained using a larger set of predictors, if they become available in future projects. However, major limitations seem to be the deficient quality of the reanalysis in this region —in agreement with Brands et al. (2012)— and the lack of skill of the seasonal forecasting systems over this area. Since, the idea for the coming future is to work with some operational seasonal forecasting model/s (e.g. ECMWF System4, but still to decide), this potential gain of skill will be further explored in the future.

Finally, all the results have been include in

---

[6]See the user documentation for more details on the methods: https://www.meteo.unican.es/downscaling/doc/UserGuide.pdf

the QWeCI statistical downscaling portal and can be downloaded for further analysis from http://www.meteo.unican.es/downscaling/qweci using the user/password qweci/qweci.

8   Acknowledgements

References

BRANDS, S AND GUTIÉRREZ, JM AND HERRERA, S AND COFIÑO, AS, 2012: *On the use of reanalysis data for downscaling*, Journal of Climate, doi:{10.1175/JCLI-D-11-00251.1}.

DEE, D.P., UPPALA, S.M., SIMMONS, A.J., BERRISFORD, P., POLI, P., KOBAYASHI, S., ANDRAE, U., BALMASEDA, M.A., BALSAMO, G., BAUER, P., BECHTOLD, P., BELJAARS, A.C.M., VAN DE BERG, L., BIDLOT, J., BORMANN, N., DELSOL, C., DRAGANI, R., FUENTES, M., GEER, A.J., HAIMBERGER, L., HEALY, S.B., HERSBACH, H., HLM, E.V., ISAKSEN, L., KLLBERG, P., KHLER, M., MATRICARDI, M., MCNALLY, A.P., MONGE-SANZ, B.M., MORCRETTE, J.-J., PARK, B.-K., PEUBEY, C., DE ROSNAY, P., TAVOLATO, C., THPAUT, J.-N., VITART, F., 2011: *The ERA-Interim reanalysis: configuration and performance of the data assimilation system*, Quarterly Journal of the Royal Meteorological Society, **137**, 553–597, doi:10.1002/qj.828.

DEME, A., VILTARD, A., DE FÉLICE, P., 2002: *Daily Precipitation Forecasting in Dakar Using the NCEP–NCAR Reanalyses*, Journal of Clmate, **16**, 0882–8156.

ELTAHIR, E.A.B., GONG, C., 1996: *Dynamics of wet and dry years in West Africa*, Journal of Climate, **9**, 1030–1042.

FONTAINE, B., JANICOT, S., MORON, V., 1995: *Rainfall Anomaly Patterns and Wind Field Signals over West Africa in August (1958–1989)*, Journal of Climate, **8**, 1503–1510.

MO, K.C., THIAW, W.M., 2002: *Ensemble canonical correlation prediction of precipitation over the Sahel*, Geophysical Research Letters, **29**, 11–1.

MORON, V., ROBERTSON, A.W., WARD, M.N., NDIAYE, O., 2008: *Weather types and rainfall over Senegal. Part II: Downscaling of GCM simulations*, Journal of Climate, **21**, 288–307.

PAETH, H., BORN, K., PODZUN, R., JACOB, D., 2005: *Regional dynamical downscaling over West Africa: Model evaluation and comparison of wet dry years*, Meteorologische Zeitschrift, **14**, 349–367.

PENLAP, E.K., MATULLA, C., VON STORCH, H., KAMGA, F.M., 2004: *Downscaling of GCM scenarios to assess precipitation changes in the little rainy season (March-June) in Cameroon*, Climate Research, **26**, 85–96, doi:10.3354/cr026085.

ROTSTAYN, L.D., LOHMANN, U., 2002: *Tropical rainfall trends and the indirect aerosol effect*, Journal of Climate, **15**, 2103–2116.

ROWELL, D.P., 2003: *The impact of Mediterranean SSTs on the Sahelian rainfall season*, Journal of Climate, **16**, 849–862.

WEISHEIMER, A., DOBLAS-REYES, F. J., PALMER, T. N., ALESSANDRI, A., ARRIBAS, A., DÉQUÉ, M., KEENLYSIDE, N., MACVEAN, M., NAVARRA, A., ROGEL, P., 2009: *ENSEMBLES: A new multi-model ensemble for seasonal-to-annual prediction. Skill and progress beyond DEMETER in forecasting tropical Pacific SSTs*, Geophysical Research Letters, **36**, 36, doi: 10.1029/2009GL040896.

ZHENG, X., ELTAHIR, E.A.B., EMANUEL, K.A., 1999: *A mechanism relating tropical Atlantic spring sea surface temperature and west African rainfall*, Quarterly Journal of the Royal Meteorological Society, **125**, 1129–1163, doi:10.1002/qj.1999. 49712555604.